Wind speed sensor data processing based on Kaman Vortex Street principle

Wenjing Xie, *Shejiao* Hu*, *Zhao* Niu, *Changyong* Wei, *Xiaolong* Yang and *Bin* Zhang

Department of Computer and information, Hefei University of Technology, 485 Danxia road, Shushan district, Hefei city, Anhui province, China.

Abstract. Wind speed is one of the important monitoring parameters to ensure mine safety. The commonly used mine wind speed sensor can be divided into ultrasonic type, impeller type and hot wire type according to the design principle. The accuracy of the latter two methods is not high enough because they are susceptible to steam and coal dust in mines. The ultrasonic wind speed sensor has better measuring accuracy. In this paper, ultrasonic wind speed sensor, ultrasonic sending and receiving circuit combined with ADC sampling function of the chip, to obtain the received ultrasonic amplitude change data, statistics of ultrasonic waveform changes caused by blowing, according to the number of changes in the wind speed frequency, and then calculate the real-time wind speed.

1 Theoretical foundation

1.1 Carman Vortex Street

When an infinite nonlinear resistance body is inserted vertically into the infinite flow field, two rows of alternating internal vortex rows will be generated downstream of the resistance body, and the vortex rate is proportional to the flow rate. The formula is expressed as:

$$f = S_t * V/d \tag{1}$$

According to the formula (1), when the vortex frequency f is measured, the wind speed can be obtained.

1.2 Principle of speed measurement by wind speed sensor

The ultrasonic wind speed sensor has two sound heads, one is a transmitting head, used for transmitting ultrasonic waves, one is a receiving head, used for receiving ultrasonic waves. Under the condition of no wind, the transmitting head emits a continuous and equal amplitude ultrasonic wave, and the receiving head can receive the same amplitude ultrasonic wave; When there is air flowing through the sensor, the vortex is generated, the ultrasonic wave emitted by the transmitter will collide with the vortex, the sound wave produces refraction

* Corresponding author: 1192862160@qq.com

and reflection, and the energy is lost, and the amplitude of the ultrasonic wave received by the receiver head will be reduced. When the next vortex has not yet arrived, the ultrasonic wave is normally transmitted, and the receiver receives the same amplitude sound wave normally. The number of vortices passing through the sensor is equal to the number of times the ultrasonic wave is modulated. So the modulation frequency of ultrasonic wave is the vortex frequency. From this, the real-time wind speed value can be obtained.

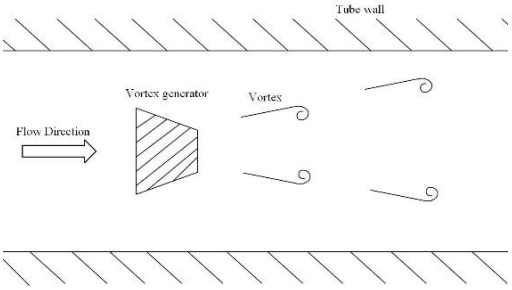

Fig. 1. Schematic diagram of Kaman Vortex Street.

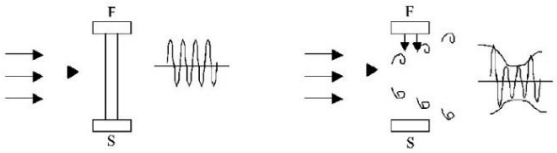

Fig. 2. Principle of vortex modulation

2 Circuit design and software design

2.1 Circuit design

2.1.1 Power section

12V power supply, through the voltage conversion chip, the 12V voltage is converted to 8V, 5V, 3.3V, 1.25V.

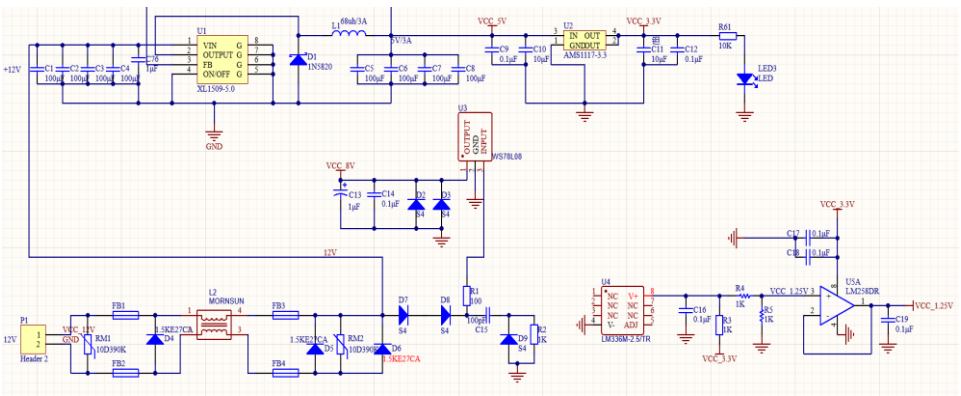

Fig. 3. Power module.

2.1.2 Ultrasonic emission part

This part is composed of an oscillating circuit and a signal driving circuit, and is powered by a separate power supply to prevent the oscillating signal from being directly coupled to the amplification circuit of the ultrasonic receiving part through the power supply network. The ultrasonic generation part is composed of integrated Schmidt inverter, RC oscillation circuit produced by capacitance and resistance.

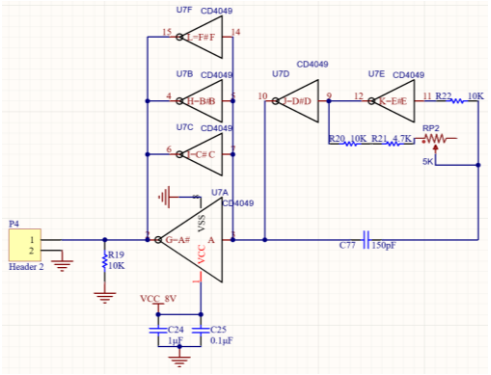

Fig. 4. Ultrasonic transmitter module.

2.1.3 Ultrasonic receiving part

The receiving part is the most important part in hardware design. It is mainly divided into three parts: frequency selection amplification, detection and subsequent amplification. Due to the need to receive wind speed acoustic signal is high resistance weak signal, and the frequency range is certain. We modulated the weak signal and the carrier signal, selected the frequency through the LC oscillation circuit, and then sent it to the operational amplifier to amplify the modulated signal. Next, the modulation signal is sent to the diode detection circuit for demodulation, and the weak signal is taken out. Finally, the weak signal is sent to the operational amplifier after amplification to the chip's ADC pin.

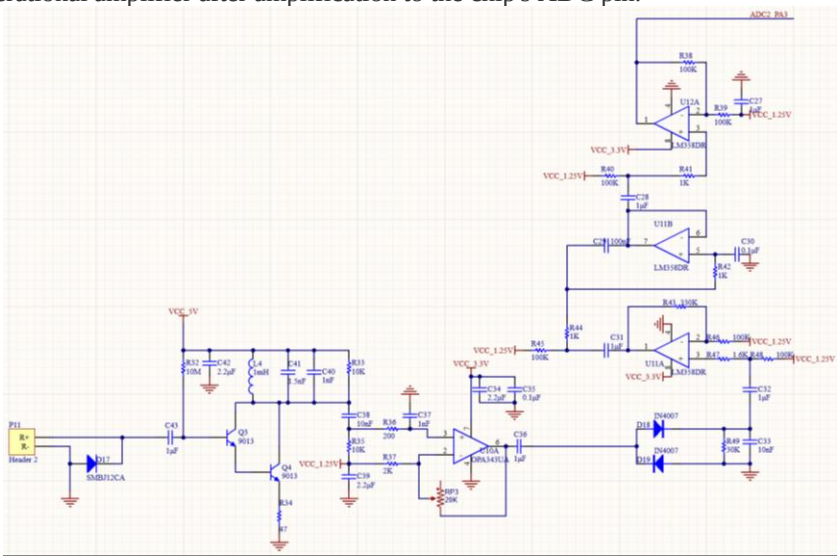

Fig. 5. Ultrasonic receiving module.

2.2 Software design

Software processing is mainly divided into two aspects: sampling range setting and anti-interference processing.

2.2.1 Sampling range setting

According to Nyquist sampling law, when the sampling frequency Fs is greater than two times of the highest frequency of the sampled signal $Fmax$, the sampled digital signal retains the information in the original signal completely. In practical applications, the sampling rate is usually set at 2.56 to 4 times the maximum frequency of the signal. The measurement range of wind speed in this paper is 0-15m/s, and the frequency range is between 0Hz-120Hz according to von Karman Formula. The sampling frequency is set as 500Hz, that is, 2ms to sample the demodulation signal once. Plan to use on-chip timer to control ADC equal interval sampling.

2.2.2 Anti-interference treatment

Because of the noise in the original sampling signal, the direct data processing will cause a large error. In this paper, the median average filtering method is used to filter certain noises. That is, the N sampling values are sorted according to their sizes, the maximum and minimum values are discarded, and the mean value of the remaining N-2 values is taken as the final sampling result. the formula is as follows :

$$\bar{X} = \frac{1}{N-2}\sum_{i=1}^{N-2} X_i \tag{2}$$

To calculate the wind speed, it is necessary to obtain the frequency modulation of ultrasonic wave. It is difficult to obtain the frequency domain information directly from the time domain, so the sampling signal can be transformed into the frequency domain by fast Fourier transform (FFT), which can understand the frequency information more intuitively. STM32 with DSP calculation library function, can be directly called. For the accuracy of FFT, the resolution is sampling frequency (Fs)/sampling points (N).

As STM32 adopts the base 4 FFT calculation, its sampling points are all exponential times of 4. According to the previous sampling frequency of 500Hz, it is proposed to use FFT of 1024 points with a resolution of about 0.5Hz. According to theoretical knowledge, the signal frequency corresponding to the point with the maximum amplitude after FFT transformation. Remove the first dc component of the array storing FFT results, search for the maximum value, return the subscript n. According to the formula (3)

$$f = (F_s/N) * n \tag{3}$$

The frequency of the sampled signal can be obtain.

3 Experimental results

The experiment simulates the tunnel environment, through the adjustable fan, using the sealed pipe to supply air to the wind speed sensor to simulate the environment in the mine. The development board is connected to the upper computer by serial port to observe the experimental data.

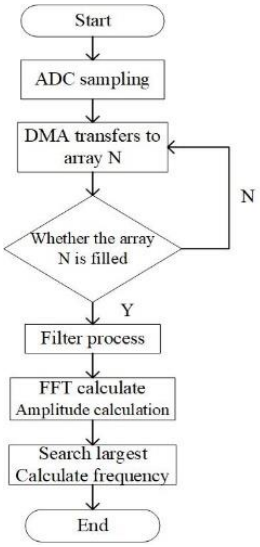

Fig. 6. Software design flowchart.

Fig. 7. Simulate tunnel environment.

Turn on the fan and adjust the blower gear. It can be observed that the wind speed printed by the serial port gradually rises.

Fig. 8. Experimental simulation results.

4 Conclusion

In this paper, median filter and FFT algorithm are used to measure wind speed. There is still a lot of room for improvement. For example, the maximum frequency range fluctuates in the process of wind speed change, and the same sampling rate and sampling points are not very good for the performance of signal restoration in the case of low wind speed. Too much sampling data may cause space waste. In the noise filtering part, the median filter is adopted, and a better anti-noise filtering algorithm can be introduced in the subsequent improvement.

References

1. B.Ovgor , S-K. Lee , S.Lee. J. Mech. Sci. Technol, **26** (2012)
2. S. V. Bozhokin et al, Biophysics , **57** (2012)
3. G. G. Gevorkyan, A.Kamont, J. Contemp, Math. Anal.-Armen. Aca. **47** (2012)
4. J.Chen , M.Wu, Asia-Pac. J. Atmos. Sci. 48 (2012)
5. B. Lenz , U. Gaisbauer , E. Krämer. Thermophys. Aeromechanics, **14** (2007)
6. A. J. Smits, K. Hayakawa, K. C. Muck, Exp. Fluids, **1** (1983)
7. M. A. Kegerise, E. F. Spina, Exp. Fluids, **29** (2000)
8. S. Franchini, A. Sanz-Andrés, A. Cuerva, Exp. Fluids, **42** (2007)
9. A.A.Quaranta et al, J Phys E, **18** (1985)
10. Z.Q.Sun, J.M.Zhou, P.Zhou. J. Cent. South Univ. Technol. **13** (2006)
11. P.Brassier, B.Hosten, F.Vulovic. Flow Meas. Instrum. **3** (2001)